Intercalation Leads to Inverse Layer Dependence of Friction on Chemically Doped MoS_2

Ogulcan Acikgoz,[1*] Enrique Guerrero,[2*] Alper Yanilmaz,[3*] Omur E. Dagdeviren,[4] Cem Çelebi,[3†] David A. Strubbe,[2†] and Mehmet Z. Baykara[1†]

[1]Department of Mechanical Engineering, University of California Merced, Merced, California 95343, USA

[2]Department of Physics, University of California Merced, Merced, California 95343, USA

[3]Department of Physics, Izmir Institute of Technology, Izmir 35430, Turkey

[4]Department of Mechanical Engineering, École de technologie supérieure, University of Quebec, Quebec H3C 1K3, Canada

* These authors contributed equally to this work.

† Corresponding authors: cemcelebi@iyte.edu.tr, dstrubbe@ucmerced.edu, mehmet.baykara@ucmerced.edu

Abstract

We present results of atomic-force-microscopy-based friction measurements on Re-doped molybdenum disulfide (MoS_2). In stark contrast to the widespread observation of decreasing friction with increasing number of layers on two-dimensional (2D) materials, friction on Re-doped MoS_2 exhibits an anomalous, i.e., *inverse* dependence on the number of layers. Raman spectroscopy measurements combined with *ab initio* calculations reveal signatures of Re intercalation. Calculations suggest an increase in out-of-plane stiffness that inversely correlates with the number of layers as the physical mechanism behind this remarkable observation, revealing a distinctive regime of puckering for 2D materials.

Keywords: atomic force microscopy, chemical doping, density functional theory, friction, molybdenum disulfide

1. Introduction

Friction is among the most fascinating yet least understood subjects in classical mechanics. Despite its prevalence in mechanical systems, systematic studies aimed at uncovering the underlying physical mechanisms on fundamental length scales became only possible with the advent of modern experimental tools such as the atomic force microscope (AFM) [1, 2]. While such methods provide outstanding resolution in space and force, a comprehensive physical picture of frictional processes remains yet to be formed, mainly because the phenomenon is a complex function of the multi-scale structural, mechanical and chemical properties of the surfaces involved, as well as environmental factors such as temperature and humidity [3].

The discovery of the exotic electronic properties exhibited by graphene about fifteen years ago [4] and the ensuing boom in two-dimensional (2D) materials [5, 6] led to new avenues in fundamental friction research. In particular, the atomically smooth and chemically inert surfaces exposed by the majority of 2D materials provide a simplified platform on which AFM-based friction experiments can be performed [7]. Such studies also exhibit practical relevance, as 2D materials could potentially be employed as solid lubricants in micro- and nano-scale mechanical systems where surface-based phenomena such as friction and wear bear increasing importance, and conventional, fluid-based lubrication schemes are not feasible [8-10].

A particularly crucial discovery in AFM-based 2D material friction research is that the friction decreases with increasing number of layers, as first reported in milestone experiments by Filleter *et al.* [11] and Lee *et al*. [12]. These observations were later confirmed by a number of independent studies performed on graphene, molybdenum disulfide (MoS_2), and other 2D materials [13-15], thus establishing decreasing friction with increasing number of layers as a seemingly universal characteristic of 2D materials. Among various theories proposed to

explain the underlying physical mechanisms, the one that gained the most traction in the literature is the *puckering* effect [12]. In particular, it is proposed that the sharp AFM tip sliding on a 2D material leads to the formation of a *pucker* (bulge) ahead of the tip, thus leading to an increase in contact area and enhanced friction. As the number of layers increases, the sample's bending stiffness increases as it would for a thicker beam, resulting in the suppression of the pucker and thus decreasing friction [16]). Puckering is also reduced by increased adhesion to a substrate which hinders out-of-plane deformation, and thus reduces the layer dependence [17]. While the idea of puckering, which has been studied in detail via computational approaches [16], can explain the trend of decreasing friction with increasing number of layers, other theories have also been proposed to explain the trend, ranging from a suppression of electron-phonon coupling (and thus a reduction in energy dissipation) [11] to decreasing surface roughness [13] with increasing number of layers. On the other hand, no direct studies have been conducted to address the question of whether this apparently ubiquitous layer-dependence trend of friction on 2D materials can be suppressed or even reversed through certain approaches, including but not limited to the application of strain [18], electrostatic fields [19, 20], and chemical doping [21].

Motivated as above, we report here, by way of AFM-based friction measurements performed on rhenium (Re)-doped MoS_2, the observation of *inverse* layer dependence of friction, in stark contrast to the seemingly universal trend of decreasing friction with increasing number of layers of 2D materials. Raman spectroscopy measurements interpreted by *ab initio* density functional theory (DFT) calculations indicate that the Re dopants are intercalated between MoS_2 layers. DFT additionally reveals that Re intercalants lead to an increase in out-of-plane stiffness, an effect that decreases with increasing number of layers, but that the dopants do not significantly affect the interaction of an AFM tip with a rigid, flat MoS_2 surface.

2. Results and discussion

2.1. AFM-based friction measurements on undoped and Re-Doped MoS_2

We started our investigation by studying the layer dependence of friction on undoped MoS_2. As demonstrated in figure 1 (a) and (b) for a stair-like flake that progressively features one-to five-layer regions, the layer-dependence results obtained via friction force maps recorded on undoped MoS_2 are in harmony with previous experimental studies in the literature [12]. In particular, the friction force is monotonically decreasing with increasing number of layers, pointing toward an enhanced solid lubrication effect with increasing thickness.

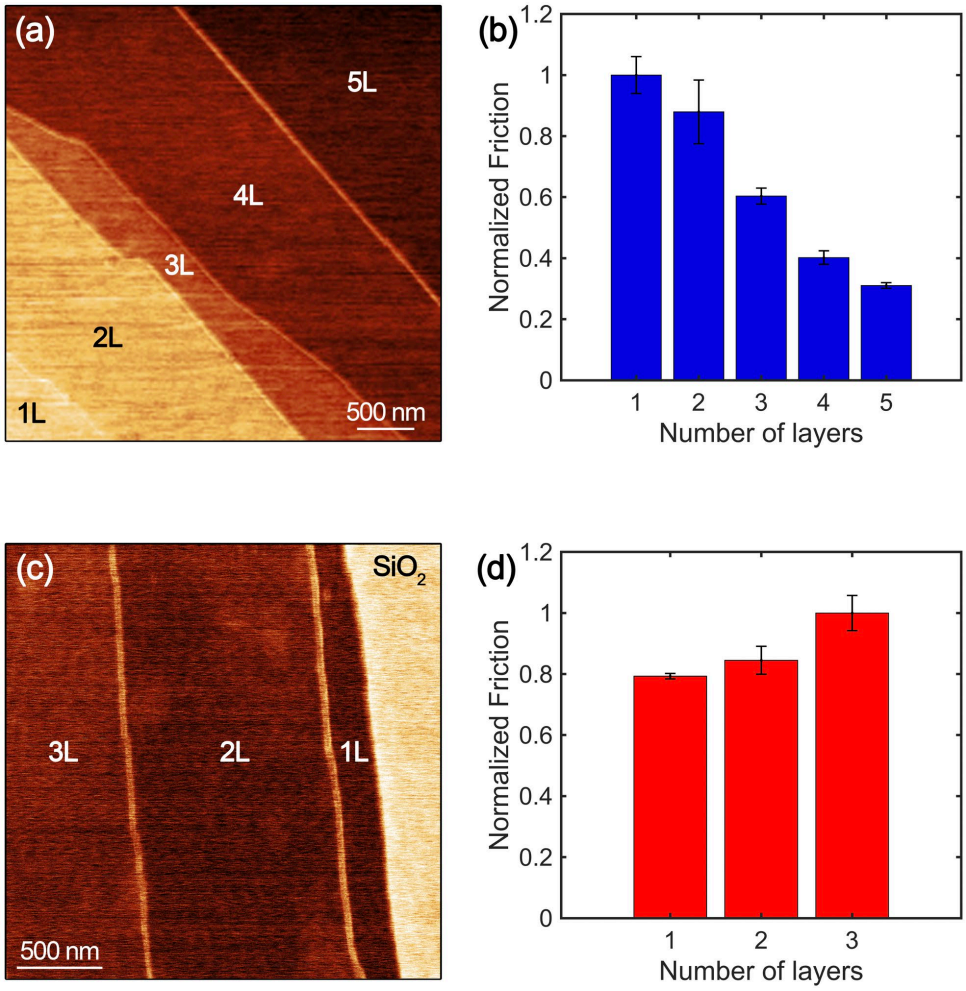

Figure 1. AFM-based friction measurements on undoped and Re-doped MoS_2 flakes. (a) Friction force map obtained on an undoped MoS_2 flake with 1, 2, 3, 4, and 5 layers (1L, 2L, 3L, 4L, and 5L, respectively) situated on a SiO_2 substrate. (b) Friction on undoped MoS_2 areas

with different number of layers. Friction is normalized to the value obtained on the 1L area. (c) Friction force map obtained on a Re-doped MoS_2 flake with 1, 2, and 3 layers (1L, 2L, and 3L, respectively), situated on a SiO_2 substrate. (d) Friction on Re-doped MoS_2 areas with different number of layers. Friction is normalized to the value obtained on the 3L area.

Unlike undoped MoS_2, AFM-based friction measurements on Re-doped MoS_2 reveal that Re-doped flakes exhibit a completely unexpected inverse layer dependence of friction. In particular, results reported in figure 1 (c) and (d) for a Re-doped MoS_2 flake with one-, two-, and three-layer regions show a striking contrast to those in figure 1 (a) and (b). Specifically, while solid lubrication is still achieved with Re-doped MoS_2 (i.e. the friction force recorded on Re-doped MoS_2 is always lower than the underlying SiO_2 substrate), single-layer Re-doped MoS_2 exhibits the lowest friction force and the friction force increases with the number of layers, in violation of the seemingly universal rule of decreasing friction with increasing number of layers.

To confirm the anomalous results obtained on Re-doped MoS_2 and ensure that the findings are not specific to one flake, measurements were repeated on a different Re-doped MoS_2 flake with two-, eleven-, thirteen-, fourteen- and fifteen-layer regions. The results (figure 2) demonstrate a similar overall trend: increasing friction with number of layers, with the trend reaching an apparent saturation after fourteen layers. By comparing to friction on the SiO_2 substrate, we find that Re-doped MoS_2 exhibits generally lower friction than pristine MoS_2, and the highest number of layers have friction comparable to pristine MoS_2 (Table S1).

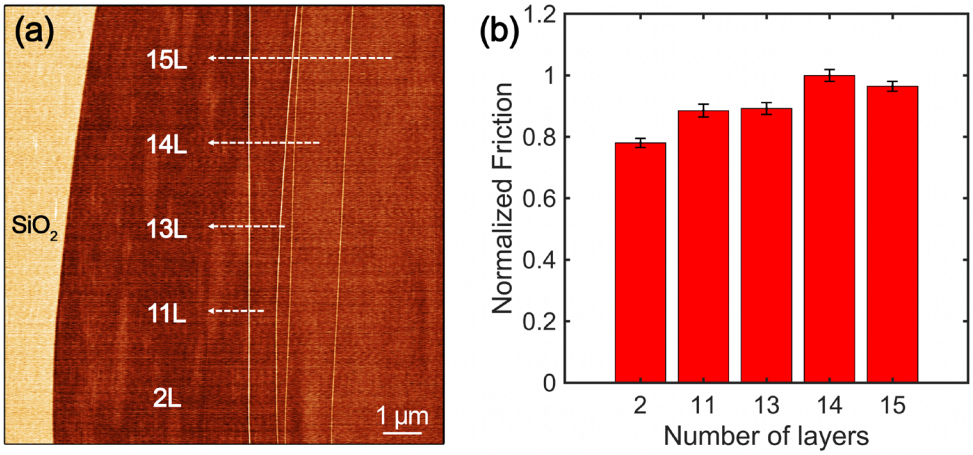

Figure 2. AFM-based friction measurements on a Re-doped MoS_2 flake. (a) Friction force map obtained on a Re-doped MoS_2 flake with 2, 11, 13, 14, and 15 layers (2L, 11L, 13L, 14L, and 15L, respectively), situated on a SiO_2 substrate. (b) Friction on Re-doped MoS_2 areas with different number of layers. Friction is normalized to the value obtained on the 14L area.

It needs to be pointed out that an increasing friction trend with increasing number of layers was shown once before, on undoped MoS_2 samples [15], and attributed to an exceptionally large AFM probe apex. In particular, the large apex led to a weakening of the puckering effect such that the layer dependence trend is now dominated by the corrugation of the potential-energy landscape experienced by the probe apex as it slides over different samples. On the other hand, the "regular" results obtained on undoped MoS_2 using the same AFM probe in our experiments (figure 1(a) and (b)) exclude a possible link between probe characteristics and the unusual findings on Re-doped MoS_2. The sharpness of the step edges in the friction maps provide further proof for the absence of an exceptionally blunt apex. Based on these observations, we are confident that the observed anomalous trend is intrinsic to Re-doped MoS_2 and not probe-dependent.

2.2. Raman spectroscopy on undoped and Re-Doped MoS_2

To explore the physical reasons behind the observation of an inverse layer-dependence of friction on Re-doped MoS_2, we first checked the potential presence of unexpected trends in

adhesion and roughness with increasing number of layers. The results of these investigations do not yield any significant trends in the layer-dependent behavior of adhesion and roughness that would explain the anomalous trend in friction we observe for the Re-doped samples (figure S1-S2). Subsequently, we performed Raman spectroscopy measurements on single-layer, few-layer (i.e., with less than 10 layers) and bulk flakes of undoped and Re-doped MoS_2, the results of which are summarized in figure 3. The main conclusions from these measurements can be described as follows: (i) the separation in frequency between the E_{2g} and A_{1g} modes (19 cm^{-1}, 23 cm^{-1}, and 25 cm^{-1} for single-layer, few-layer and bulk MoS_2 regions, respectively) decreases with decreasing thickness in accordance with the literature[22]; (ii) the spectra of Re-doped MoS_2 are devoid of peaks associated with the formation of ReS_2 (an E_{2g} peak at 163 cm^{-1} and an A_{1g}-like peak at 213 cm^{-1}), ruling out phase segregation as a result of Re doping [23]; (iii) there is a significant decrease in the intensity of the E_{2g} and A_{1g} peaks for all Re-doped samples (calibrated against the intensity of the reference Si peak at 521 cm^{-1}) when compared with the undoped ones; and (iv) the two predominant Raman-active modes of MoS_2 (the E_{2g} mode, which arises from the in-plane opposite vibration of two S atoms against a Mo atom, and the A_{1g} mode, which corresponds to the out-of-plane vibrations of S atoms in opposite directions) [24] are observed in all samples, with small red shifts in the few- and many-layer cases.

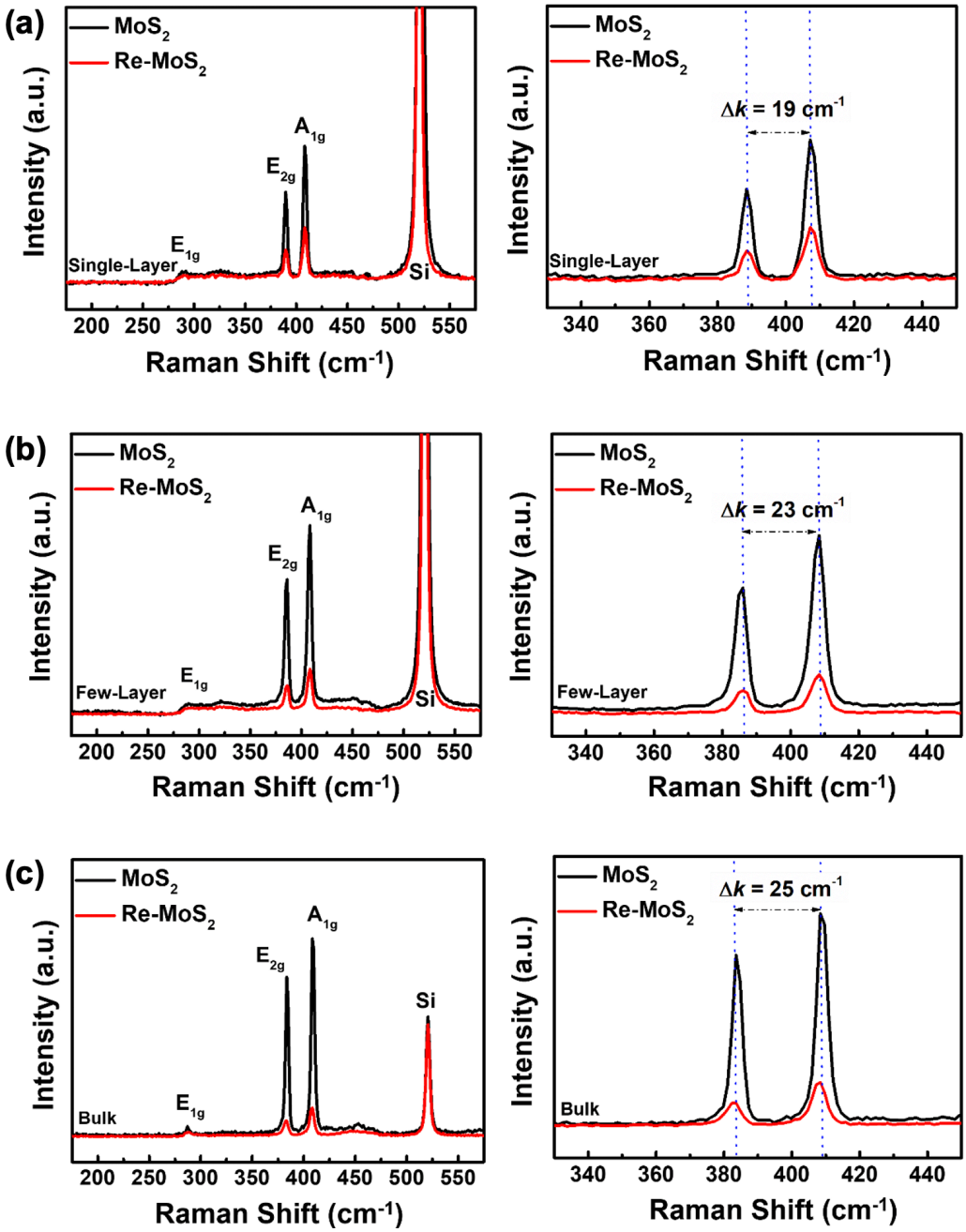

Figure 3. Raman spectroscopy on undoped and Re-doped MoS_2.. Raman spectra of (a) single-layer, (b) few-layer and (c) bulk samples of undoped and Re-doped MoS_2. The panels on the right are zooms on the regions that contain the E_{2g} and A_{1g} peaks of MoS_2. Δk indicates the wavenumber spacing between the E_{2g} and A_{1g} peak positions, which are themselves highlighted by the dotted blue lines.

2.3. DFT Calculations

The observations about intensity changes (iii) and peak shifts (iv) allow us to infer the doping site for Re. For transition-metal dichalcogenides, particularly in many-layer form, determination of doping site is a significant experimental challenge, only definitively resolved in a few cases [25, 26]. Intercalation between the layers, and substitution for the chemically similar Mo, are the most typical sites for a transition-metal dopant such as Re in MoS_2, and are the most thermodynamically favorable for Re [27]. We performed plane-wave DFT calculations with Quantum ESPRESSO [28, 29] of Raman spectra [30] using the approximation we developed for metallic doped systems [27]). We studied bulk (multi-layer) MoS_2, undoped and with Re in tetrahedral (t-) intercalation and Mo substitution sites, to identify frequency shifts in the two prominent peaks (figure 4). t-intercalation has a red shift in both peaks, consistent with the measurements in figure 3(c), whereas Mo substitution has a blue shift for E_{2g}, thus pointing to t-intercalation as the predominant dopant site. This calculated blue shift matches Raman measurements by Gao *et al.* for a monolayer MoS_2 sample believed to have Mo substitution on the basis of electron microscopy and photoemission [31]. Apart from the peak shifts, the significant decrease in peak intensities relative to undoped MoS_2 is consistent with similar observations reported before for MoS_2 intercalated with Co [32] and Li [33]. This decrease was also seen for intercalation into other 2D materials such as $MoSe_2$, WSe_2, WS_2, and graphene [32]. Our DFT calculations point to a decrease but of lesser magnitude for t-intercalation, but also for Mo-substituted MoS_2; and little effect was seen in DFT calculations of Ni-intercalated MoS_2 [34]. As a result, the mechanism for the experimental observations is unclear and may relate to dynamical effects in the Raman tensor. Regardless of mechanism, the decreased Raman intensities together with the peak redshifts indicate that the Re dopants are primarily intercalated in the sample. We note that two layers at minimum are required for

true intercalation, and therefore the Re-doped one-layer samples studied here may have Re atoms between the MoS_2 layer and the SiO_2 substrate, which presumably increases adhesion.

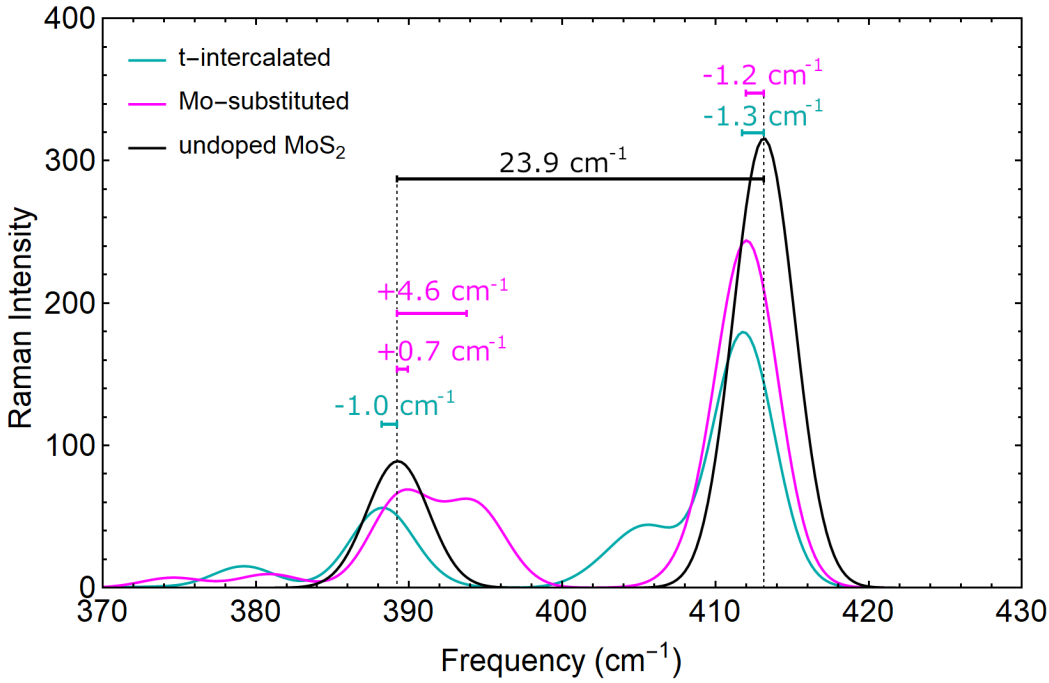

Figure 4. DFT-calculated Raman spectra for bulk (many-layer) undoped and Re-doped MoS_2 structures, using 2×2×1 (in-plane) supercells for doped MoS_2. The red shifts of E_{2g} and A_{1g} for t-intercalation best match the experimental measurements of few- and many-layer Re-doped MoS_2. Raman intensities are in units of $D^2/Å^2$-amu, per MoS_2 unit, and a Gaussian broadening of 2 cm^{-1} is used.

Now that we have determined that Re dopants primarily intercalate between MoS_2 layers, we turn our attention to establishing a physical picture that would explain the inverse layer dependence of friction observed on such samples. The usual layer dependence is due to the increase in bending stiffness with number of layers [16], which is a geometric effect that is not modified by a dopant. The bending stiffness also depends on elastic parameters such as the in-plane stiffness C_{11}, but that has little dependence on the number of layers in 2D materials [35, 36]. Our DFT calculations show that C_{11} is reduced by Re intercalation (figure S3) as the Mo-S bonds are weakened by adjacent Re-S bonding; this would reduce the bending stiffness

and increase puckering and hence friction, compared to pristine – opposite to what is observed. Instead we turn to an investigation of out-of-plane stiffness (i.e. elastic parameter C_{33}). We performed DFT calculations for bulk structures of undoped (i.e. pristine) MoS_2 as well as Re-doped MoS_2 in the t-intercalation and Mo substitution cases (see SI Sec. 2.3). The results of the calculations, summarized in figure 5(a) for supercells of decreasing size (which correspond to increasing Re concentration), show an overall increase in out-of-plane-stiffness for Re-doped MoS_2 when compared with the pristine material. Other elastic parameters, and the in-plane Young's modulus and Poisson ratio ν_{xy} which determine the bending stiffness, show only small and irregular changes (figure S3). Therefore modifications in bending stiffness cannot explain the observed trends. This stiffening effect on C_{33} is significantly more pronounced for t-intercalation than Mo-substitution, due to the formation of interlayer covalent bonds by Re [27], similar to the general increase in interlayer coupling for Ni-intercalated MoS_2 [37]. More importantly for the present discussion, the stiffening effect is proportional to the dopant concentration, suggesting a model of rigid layers connected in series by springs, in which the dopant contributes a stronger spring constant (figure 5(a), inset). In other words, the stiffening effect induced by a fixed number of Re dopants will be less pronounced for a larger number of layers.

As revealed by AFM simulations [16], there is a small volume around the AFM tip which is elastically deformed (on the order of 1 nm in lateral size), whose local elastic properties control the degree of puckering. Our samples have a low doping estimated as 0.1% of atoms, and given the exfoliation procedure from a common crystal, the flakes and terraces of different numbers of layers should have a common doping concentration. There is on average one dopant per ~30 nm^2 monolayer area (per ~15 nm^2 bilayer area, per ~2 nm^2 for 15 layers, etc.) so that the number of Re dopants in the volume below this ~ 1 nm^2 puckered area is almost always 0 or 1. When there is no dopant, the friction is as in the pristine case, but when

there is a dopant the friction is modified by this stiffness effect. The effective local dopant concentration in the volume beneath the pucker when there is a single dopant present is inversely proportional to the number of layers, resulting in a weaker stiffening effect. The friction force as measured by AFM will average over pristine-like regions and lower-friction regions with a dopant, thus giving a lower average friction force. We find possible models for this average friction which are consistent with the experimental data (SI Sec. 2.5 and figure S12), though extensive mechanical simulations would be required to establish a detailed model.

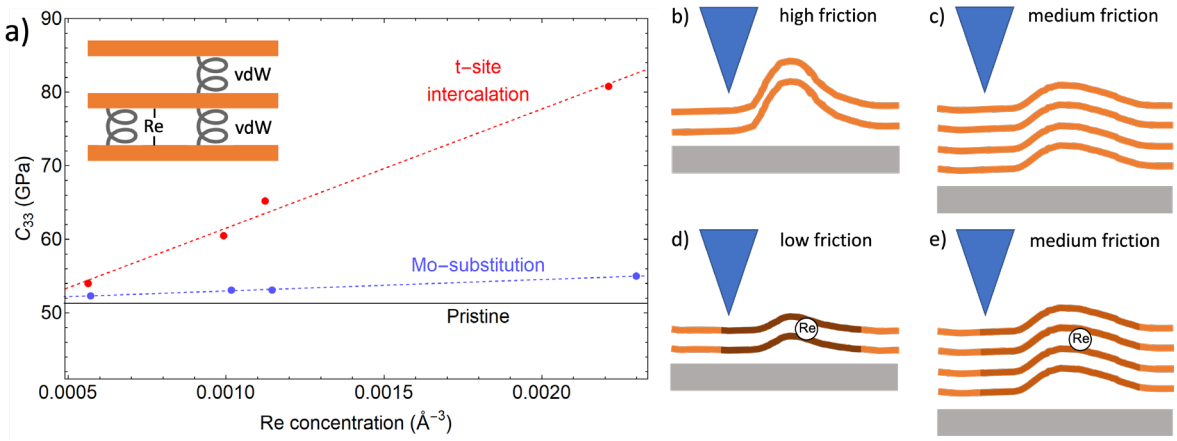

Figure 5. (a) The out-of-plane elasticity coefficient (C_{33}) for bulk Re-doped MoS_2 as a function of concentration for several different supercells with one Re per cell, showing stiffening compared to the pristine material. Inset explains the linear dependence of C_{33} on dopant concentration through a basic model of MoS_2 sheets elastically coupled by van der Waals forces, together with a single intercalated Re dopant acting as an additional, stronger "spring" due to interlayer covalent bonds. The effect of Mo-substituted Re on C_{33} is much less than that for intercalated Re. (b-d) Schematic explanation of friction trends in terms of puckering, modulated by bending stiffness (increasing with number of layers) and out-of-plane stiffness (enhanced by the presence of a Re dopant but to a smaller extent with increasing number of layers). The blue triangle is the AFM tip, the gray rectangle is the substrate, and the orange lines are MoS_2 layers, with regions stiffened by Re colored darker in proportion to the effect,

containing typically at most one Re atom. (b) undoped, few layers; (c) undoped, many layers; (d) doped, few layers; (e) doped, many layers.

While previous discussions of puckering in 2D materials have focused on the interplay of bending stiffness and substrate adhesion [16, 17], it is implicit in these studies that out-of-plane deformation in the presence of substrate adhesion is also hindered by the out-of-plane stiffness. As shown in [16], puckering involves both bending of layers and changes in interlayer distances, and therefore is controlled by not only bending stiffness but also out-of-plane elasticity. Puckering in graphene was found to have a vertical height ~1 Å, sufficient to result in significant out-of-plane strain, pulling against the underlying substrate. For multi-layers, the out-of-plane stiffness is similar to adhesion to the underlying layers, which can be modeled elastically [38], and is also related to a binding energy between layers [16]. Interplay between these properties has been previously shown to lead to unexpected phenomena such as negative coefficients of friction [39]. On the other hand, while a comprehensive model has not been established for the interplay of bending, out-of-plane stiffness, and substrate adhesion in determining puckering, it is clear that as out-of-plane stiffness increases there can be a crossover from the usual regime dominated by bending stiffness to one dominated by out-of-plane stiffness, just as a substrate-adhesion-dominated regime has been explored [17]. Our Re-doped MoS_2 samples are in this distinctive regime, as depicted in figure 5(b)-(e). Since out-of-plane stiffness reduces puckering, and for a given number of dopants in a region the increased stiffness decreases with the number of layers, therefore more puckering and consequently a higher value of friction will be observed with increasing number of layers, consistent with the experiments. Two key implications of our model which are seen in the data are: (1) friction on Re-doped MoS_2 is generally lower than on pristine MoS_2, and (2) many-layer Re-doped MoS_2 friction reaches a limit similar to pristine MoS_2 (Table S1). It should also be noted here that the degree of increase in friction from 2L to 11L reported in figure 2 is smaller than the degree

of increase in friction from 1L to 3L reported for the Re-doped flake in figure 1. Such variances in the degree of layer dependence of friction can be tentatively attributed to differences in dopant concentration or the degree of adhesion to the underlying substrate between different flakes [12]. Our model also suggests an interesting effect: in low-doped samples, friction will vary spatially on nanometer length scales based on whether a dopant is in the volume the AFM is interacting with or not, whereas in pristine samples friction will be more homogeneous; however this effect has not been resolved in the experiment since friction map pixel sizes are ~10 nm and larger than the length scale of expected variation. Additionally, the model suggests that as dopant concentration increases, and the local dopant concentration ceases to depend on number of layers, the layer dependence will be reduced or even return to the pristine trend, determined by bending stiffening by the number of layers rather than out-of-plane stiffening by the dopants; this can be a possible target of future experiments. Finally, we note that simulations have suggested that—even in the absence of puckering—out-of-plane elasticity can be a determining factor in friction on graphite [39], so there could be additional mechanisms by which out-of-plane stiffness contributes to the observed layer dependence.

For comparison to this latter explanation, we considered the possibility that the friction trends are due to changes in the potential-energy landscape, as had been indicated for the case of an exceptionally large AFM probe apex [15]. We used DFT to evaluate the friction forces that would be experienced by a model AFM tip apex [40] sliding on Re-doped MoS_2 as a function of the number of layers, in the absence of puckering (SI Sec. 2.4). The apex model consisting of 10 Si atoms (figure S4) has been used previously in the literature for AFM friction modeling [40]. We use this model for simplicity, out of various possible structures for the tip apex which could also potentially include oxygen or hydroxyl passivation. It is very difficult to determine the structure experimentally, and we are looking for trends rather than quantitative comparisons to experiment, which are expected to be similar regardless of detailed structure or

composition of the tip apex. In our calculations with this model, we find that friction forces *decrease* as the first few layers are added, opposite to the experimental dependence for few layers, and then saturate after these first few layers unlike the experiments. Moreover, the friction forces on Re-doped MoS_2 are substantially *higher* than on undoped MoS_2 (figure S10-S11). These findings are at significant variance with the experiments and thereby leave alterations to the degree of puckering (which overwhelm the effect of the potential-energy landscape) as the most likely explanation for the experimental observations.

3. Conclusions

We presented here the remarkable observation of an inverse layer dependence of friction on Re-doped MoS_2, in violation of the general understanding that friction on 2D materials decreases with increasing number of layers. Informed by Raman spectroscopy measurements and *ab initio* calculations, we proposed a mechanism of decreasing out-of-plane stiffness with increasing number of layers for a given number of intercalated dopants, which leads to an enhanced effect of puckering with increasing sample thickness and consequently, higher friction. Our results indicate the presence of a distinct regime of puckering where out-of-plane stiffness rather than bending stiffness or substrate adhesion is the decisive factor. This study opens the way for selective tuning of friction in micro- and nano-scale mechanical systems, by the combined use of undoped 2D materials and those with intercalated dopants (which are most probably not limited to the Re-doped MoS_2 system investigated here). On the other hand, more work will need to be conducted to determine if there is a limit to the friction increase with increasing number of layers (as suggested by the data presented in figure 2, and our model) and the effect of doping concentration.

Data Availability. The data that support the findings of this study are available from the corresponding authors upon request.

Acknowledgements. This work was supported by the Merced nAnomaterials Center for Energy and Sensing (MACES) via the National Aeronautics and Space Administration (NASA) Grant Nos. NNX15AQ01 and NNH18ZHA008CMIROG6R. We thank Sefaattin Tongay for graciously providing the Re-doped MoS_2 samples. O.E.D. acknowledges Canada Economic Development Fund, Natural Sciences and Engineering Research Council of Canada, and Le Fonds de Recherche du Québec - Nature et Technologies. Computational resources were provided by the Multi-Environment Computer for Exploration and Discovery (MERCED) cluster at UC Merced, funded by National Science Foundation Grant No. ACI-1429783, and by the National Energy Research Scientific Computing Center (NERSC), a U.S. Department of Energy Office of Science User Facility operated under Contract No. DE-AC02-05CH11231.

References

[1] Binnig G, Quate C F, and Gerber C 1986 Atomic Force Microscope *Phys. Rev. Lett.* **56** 930.

[2] Mate C M, McClelland G M, Erlandsson R and Chiang S 1987 Atomic-scale friction of a tungsten tip on a graphite surface *Phys. Rev. Lett.* **59** 1942.

[3] Vanossi A, Dietzel D, Schirmeisen A, Meyer E, Pawlak R, Glatzel T, Kisiel M, Kawai S, and Manini N 2018 Nanotribology *Beilstein J. Nanotechnol.* **9** 1995.

[4] Novoselov K S, Geim A K, Morozov S V, Jiang D, Zhang Y, Dubonos S V, Grigorieva I V, and Firsov A A 2004 Electric field effect in atomically thin carbon films *Science* **306** 666.

[5] Novoselov K S, Fal'ko V I, Colombo L, Gellert P R, Schwab M G, and Kim K 2012 A roadmap for graphene *Nature* **490** 192.

[6] Das S, Robinson J A, Dubey M, Terrones H, and Terrones M 2015 Beyond Graphene: Progress in Novel Two-Dimensional Materials and van der Waals Solids *Annu. Rev. Mater. Res*. **45** 1.

[7] Akinwande D *et al.* 2017 A review on mechanics and mechanical properties of 2D materials—Graphene and beyond *Extreme Mech. Lett.* **13** 42.

[8] Kim K S, Lee H J, Lee C, Lee S K, Jang H, Ahn J H, Kim J H, and Lee H J 2011 Chemical Vapor Deposition-Grown Graphene: The Thinnest Solid Lubricant *ACS Nano* **5** 5107.

[9] Berman D, Erdemir A, and Sumant A V 2014 Graphene: a new emerging lubricant *Mater. Today* **17** 31.

[10] Berman D, Erdemir A, and Sumant A V 2018 Approaches for Achieving Superlubricity in Two-Dimensional Materials *ACS Nano* **12** 2122.

[11] Filleter T, McChesney J L, Bostwick A, Rotenberg E, Emtsev K V, Seyller T, Horn K, and Bennewitz R 2009 Friction and Dissipation in Epitaxial Graphene Films *Phys. Rev. Lett.* **102** 086102.

[12] Lee C, Li Q Y, Kalb W, Liu X Z , Berger H, Carpick R W, and Hone J 2010 Frictional Characteristics of Atomically Thin Sheets *Science* **328** 76.

[13] Ye Z J, Balkanci A, Martini A, and Baykara M Z 2017 Effect of roughness on the layer-dependent friction of few-layer graphene *Phys. Rev. B*. **96** 115401.

[14] Egberts P, Han G H, Liu X Z, Johnson A T C, and Carpick R W 2014 Frictional Behavior of Atomically Thin Sheets: Hexagonal-Shaped Graphene Islands Grown on Copper by Chemical Vapor Deposition *ACS Nano* **8** 5010.

[15] Fang L, Liu D M, Guo Y Z, Liao Z M, Luo J B, and Wen S Z 2017 Thickness dependent friction on few-layer MoS_2, WS_2, and WSe_2 *Nanotechnology* **28** 245703.

[16] Ye Z J, Tang C, Dong Y L, and Martini A 2012 Role of wrinkle height in friction variation with number of graphene layers *J. Appl. Phys*. **112** 116102.

[17] Li Q Y, Lee C, Carpick R W, and Hone J 2010 Substrate effect on thickness-dependent friction on graphene *Phys. Status Solidi B* **247** 2909.

[18] Zhang S, Hou Y, Li S Z, Liu L Q, Zhang Z, Feng X Q, and Li Q Y 2019 Tuning friction to a superlubric state via in-plane straining *Proc. Natl. Acad. Sci. U.S.A*. **116** 24452.

[19] Lang H J, Peng Y T, Shao G W, Zou K, and Tao G M 2019 Dual control of the nanofriction of graphene *J. Mater. Chem. C* **7**, 6041.

[20] Shi B, Gan X, Yu K, Lang H, Cao X, Zou K, and Peng, Y 2022 Electronic friction and tuning on atomically thin MoS2 *npj 2D Mater. Appl.* **6**, 39.

[21] Zhang B Z, Zhang G G, Cheng Z W, Ma F, and Lu Z B 2019 Atomic-scale friction adjustment enabled by doping-induced modification in graphene nanosheet *Appl. Surf. Sci*. **483** 742.

[22] Ji T J, Zhang A M, Fan J H, Li Y S, Wang X Q, Zhang J D, Plummer E W, and Zhang Q M 2016 Giant magneto-optical Raman effect in a layered transition metal compound *Proc. Natl. Acad. Sci. U.S.A*. **113** 2349.

[23] Aliaga J *et al.* 2019 Electrochemical hydrogen evolution over hydrothermally synthesized re-doped MoS_2 flower-like microspheres *Molecules* **24** 4631.

[24] Lee C, Yan H, Brus L E, Heinz T F, Hone J, and Ryu S 2010 Anomalous Lattice Vibrations of Single- and Few-Layer MoS_2 *ACS Nano* **4** 2695.

[25] Tedstone A A, Lewis D J, and O'Brien P 2016 Synthesis, Properties, and Applications of Transition Metal-Doped Layered Transition Metal Dichalcogenides *Chem. Mater.* **28** 1965.

[26] Vazirisereshk M R, Martini A, Strubbe D A, and Baykara M Z 2019 Solid Lubrication with MoS_2: A Review *Lubricants* **7** 57.

[27] Guerrero E and Strubbe D A 2022 arXiv:2202.12889.

[28] Giannozzi P *et al.* 2009 Quantum Espresso: a modular and open-source software project for quantum simulations of materials *J. Condens. Matter Phys.* **21** 395502.

[29] Giannozzi P *et al.* 2017 Advanced capabilities for materials modelling with Quantum Espresso *J. Condens. Matter Phys.* **29** 465901.

[30] Lazzeri M and Mauri F 2003 First-Principles Calculation of Vibrational Raman Spectra in Large Systems: Signature of Small Rings in Crystalline SiO_2 *Phys. Rev. Lett*. **90** 036401.

[31] Gao J *et al.* 2016 Transition-Metal Substitution Doping in Synthetic Atomically Thin Semiconductors *Adv. Mater.* **28** 9735.

[32] Lai H J *et al.* 2020 A self-driven approach for local ion intercalation in vdW crystals *Nanoscale* **12** 1448.

[33] Xiong F, Wang H T, Liu X G, Sun J, Brongersma M, Pop E, and Cui Y 2015 Li Intercalation in MoS2: In Situ Observation of Its Dynamics and Tuning Optical and Electrical Properties *Nano Lett.* **15** 6777

[34] Guerrero E, Karkee R, and Strubbe D A 2021 Phase stability and Raman/IR signatures of Ni-doped MoS_2 from DFT studies *J. Mater. Chem. C* **125** 13401.

[35] Lee C, Wei X D, Li Q Y, Carpick R, Kysar J W and Hone J 2009 Elastic and frictional properties of graphene *Phys. Status Solidi B* **246** 2562.

[36] Liu K *et al.* 2014 Elastic Properties of Chemical-Vapor-Deposited Monolayer MoS_2, WS_2, and Their Bilayer Heterostructures *Nano Lett.* **14** 5097.

[37] Karkee R, Guerrero E, and Strubbe D A 2021 Enhanced interlayer interactions in Ni-doped MoS_2, and structural and electronic signatures of doping site *Phys. Rev. Mater.* **5** 074006.

[38] Smolyanitsky A 2015 Effects of thermal rippling on the frictional properties of free-standing graphene *RSC Adv.* **5** 29179.

[39] Sun X , Qi Y Z, Ouyang W G, Feng X Q, and Li Q Y 2016 Recent advances in friction and lubrication of graphene and other 2D materials: Mechanisms and applications *Acta Mech. Sin.* **32** 604.

[40] Foster A S, Shluger A L, and Nieminen R M 2004 Realistic Model Tips in Simulations of nc-AFM *Nanotechnology* **15** S60.